Tetrahedron Vol. 45, No. 24, pp. 7743 to 7758, 1989
Printed in Great Britain.

0040-4020/89 $3.00+.00

AN ANALYSIS OF THE THROUGH-BOND INTERACTION USING THE LOCALIZED MOLECULAR ORBITALS WITH AB INITIO CALCULATIONS -- V
HOMO ENERGY LEVELS OF MANY PROPELLANE COMPOUNDS

Takashi Ushio, Tsuyoshi Kato, Kehong Ye, and Akira Imamura*
Department of Chemistry, Faculty of Science, Hiroshima University,
Higashisenda-machi, Nakaku, Hiroshima 730, Japan

(*Received in Japan* 17 *July* 1989)

The analysis of the through-space/bond interaction with ab initio calculation is applied to the HOMO energy levels of propellane compounds. We could investigate molecular structural factors which dominate the height of the HOMO energy levels.

INTRODUCTION

Since the concept of the "through-bond" and "through-space" interactions was first introduced by Hoffmann et al. in 1968[1], this analysis has been used for wide range of the chemistry by many theoretical and experimental chemists. Especially, the physico-chemical natures - photoelectron spectra and hyperfine structure of the ESR etc. - were analyzed in terms of the through-space/bond interactions.

In our previous papers, we proposed a method for a quantitative evaluation of the "through-bond" and "through-space" interactions using ab initio localized molecular orbitals. For example, this method could quantitatively explain the intramolecular long-range interaction between lone pair orbitals of hydrazine and so forth[2-4] or role of relay orbitals in perpendicular π-systems[5]. In the present paper, we apply the above-mentioned method to [1.1.1]propellane (Fig. 1) and [2.2.2]propellane (Fig. 2).

Both molecules have the unusual molecular structure that is remarkably strained. Namely they contain four carbon-carbon bonds which are on the same side of the plane containing the bridgehead carbons.

Before [1.1.1]- and [2.2.2]propellanes are prepared, the earliest calculations on both [1.1.1]- and [2.2.2]propellane were carried out with the extended Hückel method by Stohrer and Hoffmann.[7] They paid their

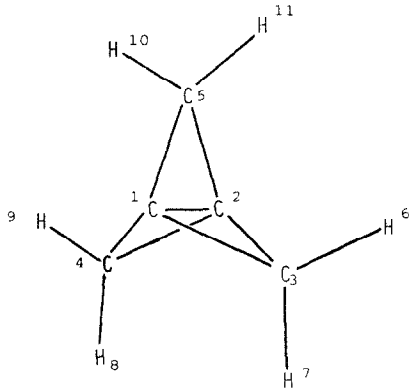

Fig.1 [1,1,1]-propellane

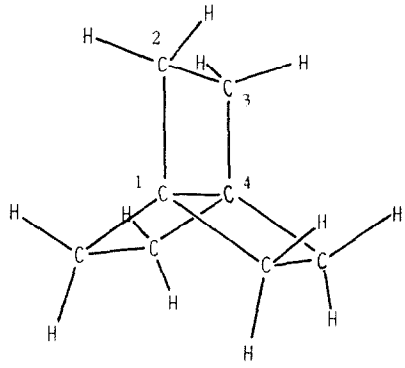

Fig.2 [2.2.2]-propellane

attentions to the characters of the bond between the bridgehead carbons in the strained tricyclic hydrocarbons, and predicted that the distance between the bridgehead carbons of [1.1.1]propellane is 1.6A. And they discussed also the nature of the interaction between bridgehead carbons in [2.2.2]propellane, that is, whether this molecule is biradical or not.

Newton and Schulman carried out the ab initio calculations on [1.1.1]propellane in lowest singlet and triplet states.[6] They predicted the lowest state to be singlet state, with a shorter bridgehead-bridgehead (central C-C) distance of 1.6A, and discussed the nature of the central C-C bond in terms of the total electron density contour map in this region, the electron density of localized molecular orbitals, and the SCF overlap populations etc.

After the success of synthesis of [1.1.1]propellane, the molecular geometry of the propellane was determined with electron-diffraction,[8] IR, and Raman spectra,[9] and the enthalpy of formation of [1.1.1]propellane was discussed[9] by many chemists. Moreover, Politzer et al. argued on the nature of the central C-C bond of [1.1.1]propellane with ab initio SCF minimum-basis set molecular wave functions,[12] and Messmer et al. also by generalized valence bond method.[13] In accordance with the high reactivity which is the character of the high strained organic compounds, the reaction of [1.1.1]propellane with free radical was reported.[11] Recently the nature of interaction between the bridgehead carbons in [1.1.1]- and [2.2.2]propellane has been investigated using ab initio TCSCF and CI wave functions by Feller and Davidson.[14] Further, the example most related to our work is the study on the photoelectron spectrum of [1.1.1]propellane by Heilbronner and Wiberg et al.[10] They found that PE spectra correspond exactly to the calculated results by ab initio MO method using polarized 6-31G* basis, etc.

In the present study, we tried to investigate the nature of the central bridgehead-bridgehead carbon's bond of [1.1.1]- and [2.2.2]propellane in terms of the through-space/bond interactions using localized molecular orbitals, and to explain how the nature of these central C-C bonds are dominated by the characteristics in the structures of the propellanes.

METHOD OF CALCULATION

The original canonical MOs (CMOs) were obtained from ab initio LCAO SCF MO calculations.[16] The basis set was the STO-3G functions with the standard scale factors developed by Pople et al.,[17] and the program GAUSSIAN 70[18] was used. The localized MOs (LMOs) were obtained from the CMOs by the procedure of Edmiston-Ruedenberg.[15] The detailed procedure of the calculations has been described in the previous paper.[2] With regard to the molecular geometric parameters of the carbon skeletons, [1.1.1]propellanes were obtained from the electron-diffraction data by Hedberg[8] and [2.2.2]propellanes were the same to those determined theoretically by Davidson et al.[14], and they are listed in Table 1 and Table 2.

Table 1. Parameter for [1.1.1]propellane

parameter	r or ∠
C-H	1.090
C_1-C_3	1.522
C_1-C_2	1.594
C_3·C_4	2.247
C_1·C_6	2.238
C_3··C_8	2.532
C_3··C_9	3.250
∠HCH	116.0
$\angle C_1C_3C_6$	116.9
$\angle C_3C_1C_4$	95.1
$\angle C_1C_3C_2$	63.1

Distances (r) in angstroms (Å)
Angles (∠) in degrees (°)

Table 2. Parameter for [2.2.2]propellane

parameter	r or ∠
C-H	1.07
C_1-C_4	1.57
C_1-C_2	1.55
C_2-C_3	1.59
∠HCH	108.1
$\angle C_1C_2H$	110.2

Distances (r) in angstroms (Å)
Angles (∠) in degrees (°)

RESULTS AND DISCUSSION

In Fig. 3, the contour map is shown for the wave function of the LMO localized between the bridgehead carbons, C_1-C_2, of [1.1.1]propellane. This corresponds to the bridgehead-bridgehead carbon bond. The electron density

of this LMO is higher in the region of the outside of the molecule than that of the inside. Since the sign of the wave function is the same between C_1 and C_2, it seems that there is the "bonding nature" between them. With regard to this, as referred to above , Politzer and Messmer et al. discussed in the past.[12-13]

In Fig. 4 the contour map is shown for the wave function of the LMO localized between the bridgehead carbons(C_1-C_4) of [2.2.2]propellane. The same problem can be discussed for it. Namely it has the high outside electron density and bonding nature, but the electron density between bridgehead carbons is slightly higher than that in [1.1.1]propellane.

The HOMO of the both propellanes are mainly localized between the bridgehead bonds. Then we investigate systematically the change of the energy level of HOMO when this bridgehead LMO interact with the other C-C bond LMOs. That is, we perform the analysis taking advantage of the symmetry, D_{3h} of [1.1.1]- and [2.2.2]propellanes.

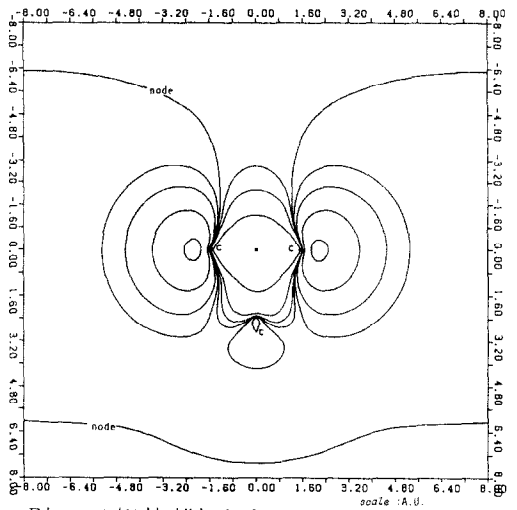

Fig. 3 Localized Molecular Orbital
[1,1,1]-propellane

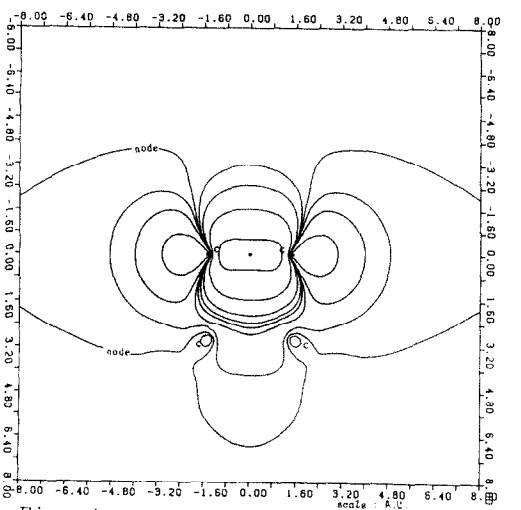

Fig. 4 Localized Molecular Orbital
[2,2,2]-propellane

[1.1.1]propellane

Interaction diagram in Fig. 5 shows the changes in the orbital energy of HOMO by the coupling with other LMOs in the occupied orbital space of [1.1.1]propellane. This figure shows how systematic analysis is carried out for the change in the HOMO energies of propellanes with D_{3h} symmetry. Namely, the energy splittings and changes are analyzed by using the symmetry of the molecule.

In interaction diagram in Fig. 5, **a** indicates the energy levels of LMOs which correspond to the central C-C bond (bridgehead bond) and the

two orbitals with A_1' symmetry in **c**. The larger the Fock matrix element is and the smaller the energy difference is, the larger the energy difference between them is.

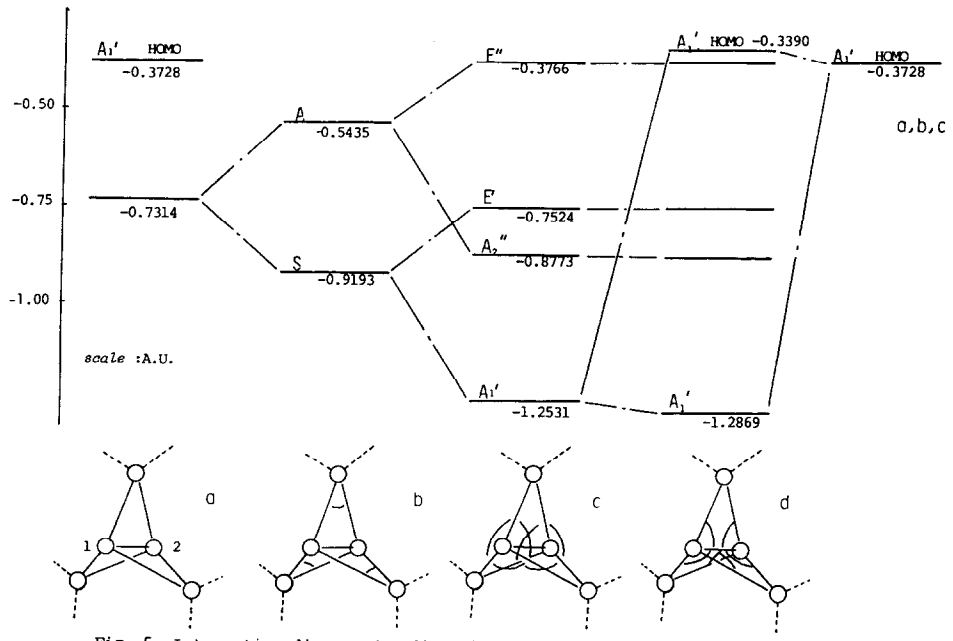

Fig. 5 Interaction diagram for [1,1,1]-propellane No.1

From the through space/bond interaction analysis described in Fig. 5, it becomes obvious that the height of HOMO level is governed by the energy difference between two A_1' orbitals in **c** and by the magnitude of the Fock matrix elements between the central C-C bond LMO and the outside skeleton C-C bond LMOs.

The magnitude of the Fock matrix element is intimately related to the structural feature around the bridgehead carbons. The energy difference between two A_1' orbitals is determined systematically as shown in **b** and **c** of Fig. 5. That is, the small Fock matrix element between two LMOs on the tops of the triangle in **b** of Fig. 5 leads to the relatively high A_1' orbital in **c**. And then it leads to small energy difference between two A_1' orbitals which give high HOMO energy level in **d**. Consequently, the Fock matrix element which is remote from the central C-C bond has a crucial role in determining the height of HOMO orbital energy.

Consequently, it is possible to obtain a propellane molecule with small ionization energy through designing the molecular structure with smaller Fock matrix element shown in **b** of Fig. 5. Another factor which determines the height of HOMO is the Fock matrix element between the central C-C bond LMO and the outside skeleton C-C bond LMO, as is described

other outside carbon skeleton bonds. In this case, all the interactions are completely cut off from each other. Six degenerate orbitals correspond to LMOs of outside carbon skeleton bonds, since all of these C-C bonds don't interact with each other and these bonds are all equivalent with each other from symmetrical point of view. These energy levels are -0.7314 au. On the other hand, the HOMO energy level is -0.3728 au(which is the energy level when the LMO of the central C-C bond doesn't interact with the other LMOs).

b in Fig. 5 shows the energy splitting for the orbitals of outside C-C bonds when the integrals are added, which corresponds to interactions between outside neighboring C-C bond LMOs on only CH_2 part at each top of triangles of the molecule . In this case, the energy levels of outside orbitals split into symmetric(S) and antisymmetric(A) orbitals for the reflection in the σ_h plane. The energy levels of S orbitals are -0.9193 au and those of A orbitals are -0.5435 au. The magnitude of this splitting depends upon the magnitudes of the interaction integral between neighboring C-C bonds LMOs on the tops of triangles containing CH_2. This is because these LMOs are degenerate when there are no interactions between the LMOs. The HOMO energy level doesn't change (-0.3728 au) because central C-C bond doesn't still interact with the other LMOs.

The next step is **c**. In addition to **b**, interaction integrals are added between the C-C bond LMOs which are neighboring at the bridgehead carbons. As a result, the outside carbon skeleton MOs separated in correspondence to the D_{3h} symmetry, because the interactions added in **c** have the symmetry of D_{3h}. Namely, the S orbitals in **b** separate into A_1' and E' orbitals and A orbitals into A_2'' and E". In this case, the energy level of A_1' orbital(bottom of **c** in Fig. 5) is -1.2531 au (and the HOMO level remains at -0.3728 au).

Finally in **d** of Fig. 5, the outside skeleton orbitals which have been separated as above interact with the central orbital localized between bridgehead carbons (C_1,C_2). The orbital localized between bridgehead carbons has the A_1' symmetry in the symmetry group of D_{3h}. Consequently the orbital localized between bridgehead carbons can interact only with the outside skeleton orbital which has the symmetry A_1' (whose energy level is -1.2531 au in **c**). Then in the interaction diagram **d** of Fig. 5, the HOMO energy level rises from -0.3728 au to -0.3390 au (the rise of energy level is 0.0338 au), while outside A_1' skeleton orbital level is -1.2869 au. A_2'', E' and E" orbitals don't change the height of their energy levels from those in **c** since they don't mix with A_1' HOMO because of the difference in the orbital symmetry. The elevation of the HOMO energy level described above depends upon not only the magnitude of the Fock matrix elements corresponding to these interactions but also the energy difference between

in **c** of Fig. 5. This factor can be controlled by designing the molecular structure around the bridgehead carbons. We are now in a position to state that the systematic through space/bond interaction analysis should be useful to obtain the indication how the molecular structure should be designed to obtain the molecule with desired physico-chemical properties such as the ionization energy with taking advantage of D_{3h} symmetry.

The HOMO orbital energy in **d** of Fig. 5 (-0.3390 au) is much higher than that for the full interaction calculation (-0.2858 au). Consequently, there must be other factors which elevate the HOMO orbital energy. In order to clarify these factors, we proceed the following analysis. Interaction diagram, Fig. 6, shows schematically the change of the HOMO energy level (upper level) and the outside carbon skeleton's A_1' orbital (lower level). The levels in **d** are the same as those in interaction diagram **d** of Fig. 5.

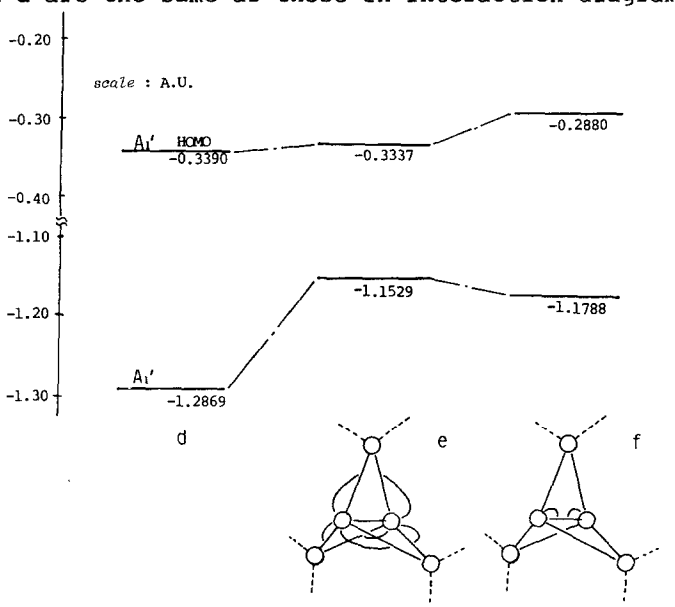

Fig. 6 Interaction diagram for [1,1,1]-propellane No.2

e in Fig. 6 is the energy level diagram, in which the interaction between bridgehead carbon's 1s orbitals and outside carbon skeleton is added to the **d** state. The HOMO energy level rises to -0.3337 au and the difference from **d** is rather small (0.0053 au). Further, in **f**, the interaction between bridgehead carbon's 1s orbitals and central C-C LMO was added to **e**. The HOMO energy level rises to -0.2880 au. The energy difference from **e** (0.0457 au) is of the same order of the interaction in **d** of Fig. 5 (0.0338 au), and it should be noteworthy that the height of the HOMO level in the state of **f** is much closer to one in the state of the full interaction (-0.2858 au). Consequently, it is the effect of the 1s orbitals

of the bridgehead carbons that is responsible for the rise of the HOMO energy level.

Although we neglected the contribution of methylene part on the top of outside skeleton's triangles , it is clear that the contributions of methylene parts should be rather small. Thus, the neglect of this contribution is quite reasonable. Since the contributions of various parts of [1.1.1]propellane molecule are remarkably dependent on the molecular geometry, so that the systematic analysis for a molecule with the D_{3h} symmetry was continued for [2.2.2]propellane in the next section.

[2.2.2]propellane

Successively, we also performed a similar systematic analysis for [2.2.2]propellane.

Interaction diagram **a** in Fig. 7 indicates the energy levels of orbitals when all C-C bonds don't interact with each other. In this case, there are six degenerated equatorial C-C bond LMOs neighboring to the central bridgehead C-C bond, whose energy levels are -0.6677 au (see the left side of the diagram). There are three degenerated LMOs which are symmetric(S) with regard to the σ_h plane. These three LMOs correspond to three C-C bonds which are parallel to the central C-C bond, whose energy levels are -0.6651 au (see the right side of the diagram). On the other hand, the central C-C bond orbital energy level is -0.5936 au shown on the farthest right side in Fig. 8.

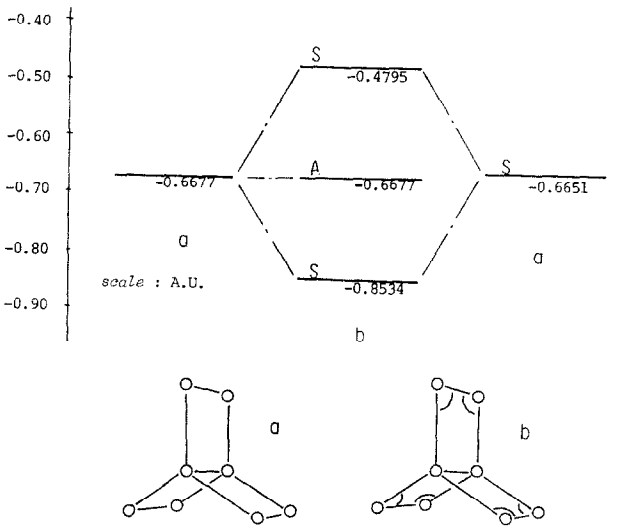

Fig. 7 Interaction diagram for [2,2,2]-propellane No.1

In **b** of Fig. 7, the energy levels are shown for the outside skeleton C-C bond orbitals when the interactions are added to C-C bonds which are nearest-neighboring on the edge of CH_2 portion. Thus, the interactions can be classified as the intra-path ones. In this case, the three symmetric orbitals which are constructed from the six degenerate C-C bond LMOs interact with the three symmetric C-C bond LMOs which are parallel to the central C-C bond. The three antisymmetric orbitals which are also constructed from the six degenerate C-C bond LMOs don't change its energy upon interaction with the three parallel C-C bond LMOs because of different symmetries. Thus, the energy levels of the outside C-C bond skeleton orbitals split into the lower symmetric (S) orbitals (-0.8534 au) , the middle antisymmetric (A) orbitals (-0.6677 au) and the higher symmetric (S) orbitals (-0.4795 au). Each of the three separated levels is all triply degenerate.

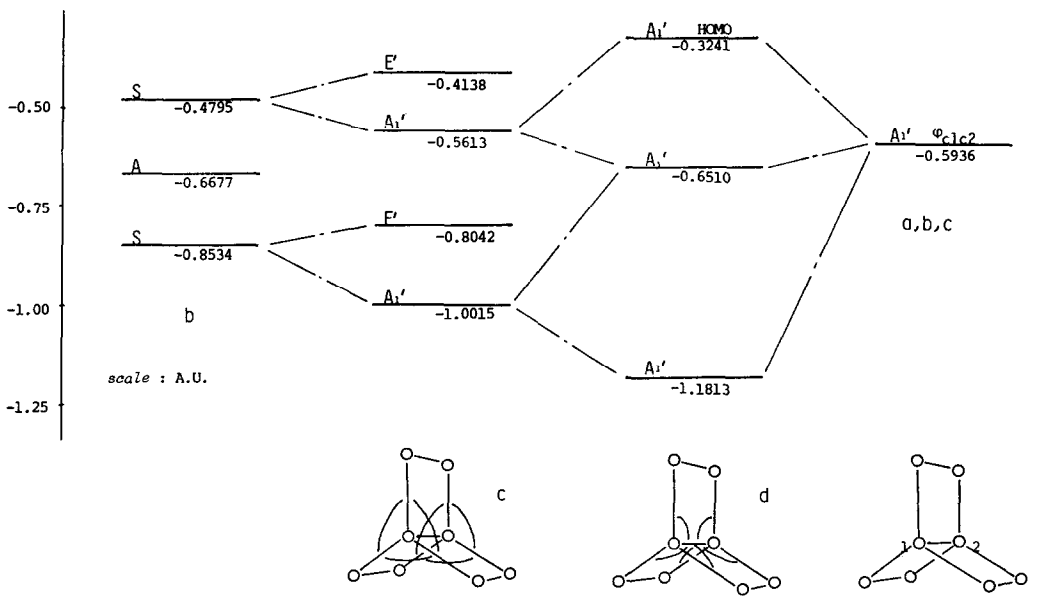

Fig. 8 Interaction diagram for [2,2,2]-propellane No.2

In order to simplify the energy level diagram that contains the orbital splitting and mixing, we pick up the central level diagram of **b** in Fig. 7, two S and A levels , and put it into Fig. 8. In Fig. 8, **b** is the same as **b** in Fig. 7.

The diagram **c** in Fig. 8 shows the energy separation when the interactions between two LMOs neighboring around the bridgehead carbon (see the figure) are added to **b**. In this case, the lower S orbitals split into

A_1' orbital (-1.0015 au) and E' orbitals (-0.8042 au). The higher orbitals also split into A_1' orbital (-0.5613 au) and E' orbitals (-0.4138 au). It should be noteworthy that the higher A_1' orbital is close to the energy level of the central C-C bond LMO.

In **d**, the central C-C bond LMO interacts with the only six LMOs which are nearest neighboring to the central C-C bond LMO at the bridgehead carbons as shown in the figure. Similarly to the case of [1.1.1]propellane, the central C-C bond A_1' orbital only mixes with both outside skeleton A_1' orbitals and rises to -0.3241 au. Namely, the energy level of the central C-C bond LMO is elevated remarkably to become the HOMO by the interaction with the higher A_1' orbital. The change in the height of the energy level is rather large (0.2695 au). The above-mentioned aspects represent that the HOMO energy level is also dominated by the interaction between the LMOs of the outside carbon skeleton on the edge of CH_2 portion shown in Fig. 7 **b**.

Similarly to [1.1.1]propellane, the factor which determines the height of the level of the higher A_1' orbital in **c**, is intimately related to the magnitude of the energy splitting in **b**. That is, if the interaction in **b** is smaller, the higher A_1' level locates lower, and the HOMO level becomes

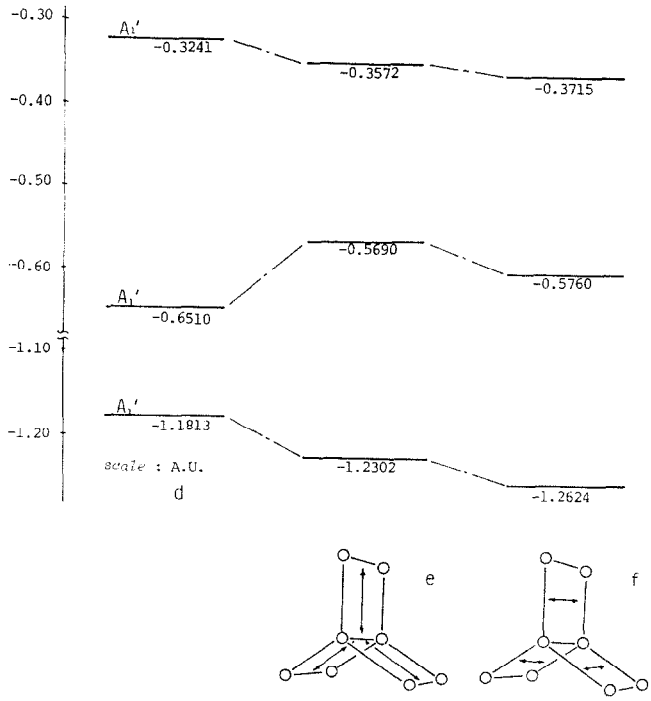

Fig.9 Interaction diagram for [2.2.2]-propellane No.3

lower. In other words, the HOMO energy level becomes lower when there are smaller Fock matrix elements between two C-C bond LMOs which are nearest-neighboring on the edge of CH_2 portion (see Fig. 7,b). Consequently, it may probably be possible to control the height of the HOMO level and thus the electron donating nature by introducing appropriate substituents on the edge CH_2 portion which give the smaller Fock matrix.

Next, we investigated the contributions of the through-space interactions to HOMO orbital energy. Fig. 9 shows the changes of the energy levels after adding two types of through space interactions which are shown by arrows in the the figure (In Fig. 9,**d** is equal to **d** in Fig. 8). **e** in Fig. 9 is the diagram in which the interactions between the outside parallel C-C bonds and the central C-C bond are added in **d**. **f** in Fig. 9 is the diagram with the interactions between the outside equatorial C-C bonds which are added to the diagram in **e**. It is obvious from this figure that these interactions lowered the HOMO energy level.

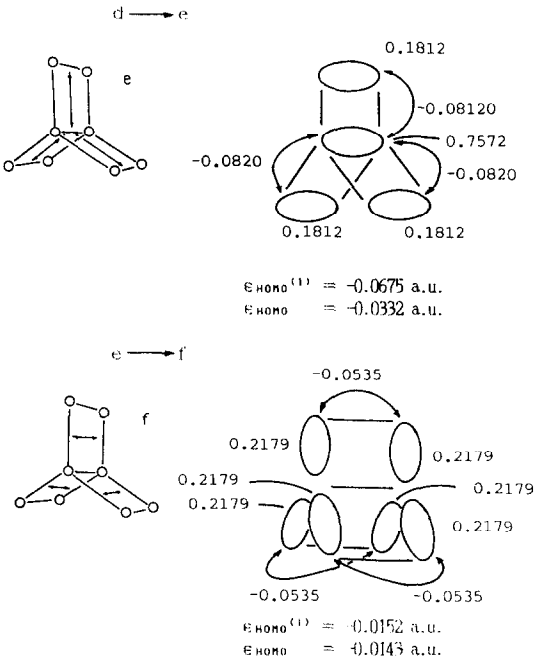

Fig.10 The coefficients and the first order Fock matrix

The tendency of the energy changes is reasonably explained by the first order perturbation energy[4,19]. This energy is given as below

$$\varepsilon_i^{(1)} = \Sigma_{r(L)}\Sigma_{s(L)}C_{ir(L)}^{(0)}C_{is(L)}^{(0)}F_{r(L)s(L)}^{(1)} \qquad (1).$$

where $C_{ir(L)}$ represents the coefficient of the r-th LMO in the i-th MO and $F_{r(L)s(L)}^{(1)}$ is the first order perturbed Fock matrix between the r-th LMO and the s-th LMO. Paying attention to the HOMO, the stabilization of the HOMO level is explained in terms of the in-phase interaction. That is, the HOMO has the same phases of wave function between the central C-C part and the outside three parallel C-C parts in **d**. Accordingly,in **e** the interactions between these parts stabilize the HOMO level since they are in-phase. On the other hand, the middle level A_1' MO in **d** has the different phases, and thus the interactions in **e** unstabilize this MO because of out-of-phase interactions.

The value and the sign of coefficients and Fock matrix elements relevant to eq.(1) are shown in Fig.10 **d→e** supporting the above-description. In this figure, the magnitudes of the HOMO energy change by the through space interaction are calculated with the usual procedure of the diagonalization (ε_{HOMO} in the figure) and with the eq.(1) of the perturbation method ($\varepsilon_{HOMO}^{(1)}$ in the figure). They are shown in comparison with each other. It is obvious that the tendency of the HOMO energy change is well reproduced by the perturbation method although the absolute magnitude deviates slightly.

The same procedure was applied to the through space interaction of Fig. 9.f. As the through space interactions are added to in-phase LMOs, we can expect the stabilization of the HOMO level. However, the magnitude of the energy change should be smaller for this interaction because of the smaller perturbed Fock matrices, $F_{r(L)s(L)}^{(1)}$, in good correspondence with the numerical results shown in Fig. 9 **e** and Fig.10 **e→f**

Until now, we have neglected the contributions of the methylene parts on the six tips of the propeller parts, but it was found that the contributions of these parts to HOMO energy are not negligibly small. Then in Fig.11, **g. h**, each LMO of the methylene parts interacts with the skeleton's LMO by through-bond interactions (pay attention to the change of the energy scale, and also to adding the all other symmetric interactions, i.e. for example in **g**, the interactions on the other tips of the propeller parts were considered). As is indicated in this figure, the HOMO level elevates by adding interactions in **g** and **h**. But when, only in the methylene parts, all possible interactions were incorporated as **i**, the HOMO is a little stabilized. Then we added the through-space interactions step by

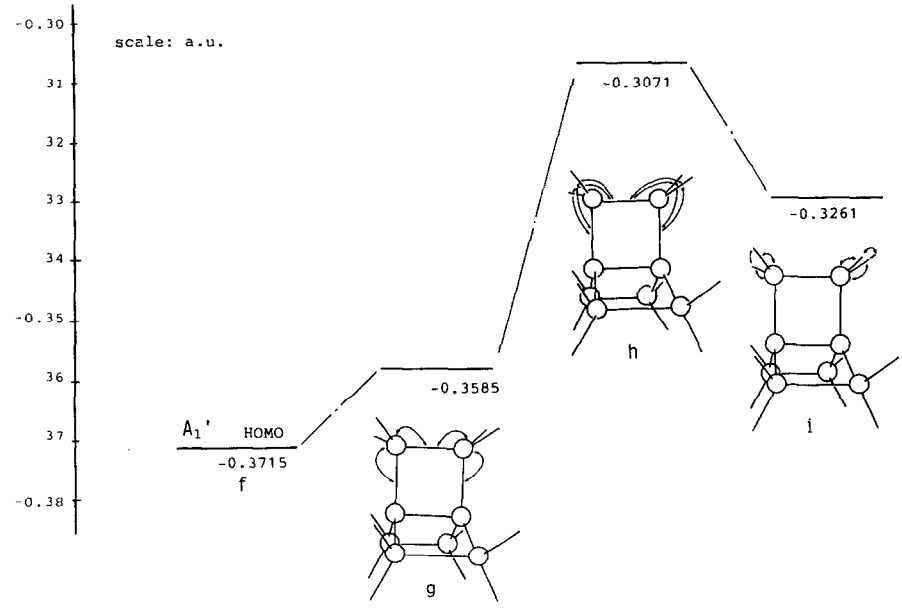

Fig.11 Interaction diagram for [2,2,2]-propellane No.4

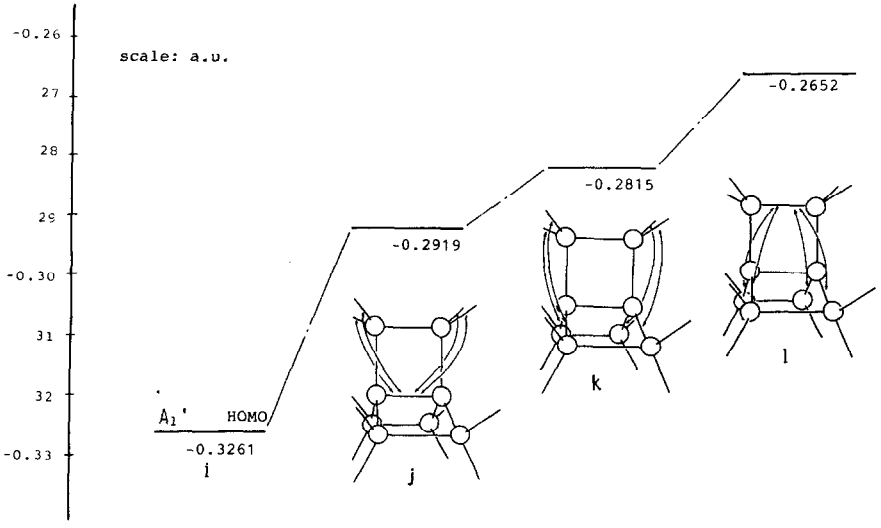

Fig.12 Interaction Diagram For [2.2.2]-propellane No.5

step as shown in **j**, **k**, **l** in Fig.12. In result, the HOMO level elevate to almost the state of the full interaction (-0.2656au).

In the previous section, it was already mentioned that the contributions of the methylene parts are negligible in [1.1.1]propellane. The difference between two propellanes is due to the character of [2.2.2]propellane in which the magnitude of the delocalization of HOMO is larger than [1.1.1]propellane. Thus it is expected that the influence of the substituents on the first ionization potential is larger for [2.2.2]propellane than one for [1.1.1]propellane.

The differences in the characters of both propellanes.

1) In [1.1.1]propellane, the central C-C bond is originally the HOMO level when all LMOs are separated. On the other hand, in [2.2.2]propellane, the central C-C bond originally locates lower and isn't HOMO, but when it interacts with the higher A_1' MO, it rise up to become HOMO by the interaction, **d** in Fig. 8. Namely, in the case of [1.1.1]propellane, the rise of HOMO is small because the energy difference between the central C-C bond A_1' MO and outside skeleton A_1' MO is larger (namely the interactions, **b** in Fig. 5 is large).

In the case of [2.2.2]propellane, the high A_1' outside skeleton MO is created because the interactions, **b** in Fig. 7 are large. With regard to [1.1.1]propellane, the rise of HOMO level in d of Fig. 5 is smaller than that of [2.2.2]propellane and central C-C bond is already HOMO. On the contrary, in [2.2.2]propellane, though the central C-C bond isn't HOMO in **b** and **c** of Fig. 8, it becomes HOMO by the large interactions in **d** of Fig 8.

In result, the difference in the height of the HOMO levels between both propellanes become very small (the HOMO level of [1.1.1]propellane and [2.2.2]propellane are -0.2858au and -0.2656au, respectively). In any cases, it is considered that the first ionization potentials of propellanes are possible to change by the introduction of appropriate substituents which change selectively the Fock matrix elements corresponding to the interactions, **b** (see the interaction diagram for [1.1.1]propellane of Fig. 5 **b** and the interaction diagram for [2.2.2]propellane of Fig. 7 **b**).

2) In the case of [2.2.2]propellane, the HOMO level slightly drops by the through-space interactions, as shown in **e**, **f** of Fig. 9. It is almost dominated by the first order perturbation energy (in-phase and out-of-phase interactions).

3) In the case of [1.1.1]propellane, the contributions of 1s shells of the carbons on the main axis are large so as to rise the HOMO level to that of the full-interaction state. On the other hand, in [2.2.2]propellane, the contributions of the methylene parts are large in the full-interaction. These results are due to larger extent of delocalization of HOMO in [2.2.2]propellane than in [1.1.1]propellane.

From this result, it can be predicted that the influence of the introduction of appropriate substituents to the first ionization potential is small in [1.1.1]propellane and large in [2.2.2]propellane.

As a whole, in both propellanes, the HOMO energy levels are dominated remarkably by the interactions of the outside skeleton. Especially, this tendency is larger in [2.2.2]propellane. The controlling of the first ionization potentials are possible by taking account of these interactions. It is concluded that these results become the serviceable data when the molecular design is performed.

CONCLUSION

For the compounds which have high symmetry, the analysis of through-space/bond interactions using the symmetry of each MO is useful. By using this method, it became clear that the interactions between C-C bonds of the outside carbon skeletons mainly influence the HOMO energy levels of both propellanes. The contributions of 1s shells in [1.1.1]propellane and that of methylene parts in [2.2.2]propellane can't be neglected so as to reach the state of the full-interaction. These results should be the serviceable data when the electron donating high strained organic compounds are planned to synthesize, and we can carry out the molecular design using these data.

ACKNOWLEDGMENT

We thank the Computer Center of the Institute for Molecular Science and the Information Processing Center of Hiroshima University for permission of the usage of HITAC M-200 and M-680H computer systems. This work was supported by a Grant-in-Aid for Scientific Research from the Ministry of Education of Japan, for which we express our gratitude.

REFERENCES

1)R. Hoffmann, A. Imamura and W. J. Hehre, J. Am. Chem. Soc., 90, 1499 (1968).
2) A. Imamura and M. Ohsaku, Tetrahedron, 37, 2191 (1981).
3) A. Imamura, A. Tachibana and M. Ohsaku, Tetrahedron, 37, 2793 (1981).
4) A. Imamura, M. Ohsaku and K. Akagi, Tetrahedron, 39, 1291 (1983).
5) K. Kanda, T. Koremoto and A. Imamura, Tetrahedron, 42, 4169 (1986).
6) M. D. Newton and J. M. Schulman. J. Am. Chem. Soc., 94:3, 773 (1972).
7) W. Stohrer and R. Hoffmann, J. Am. Chem. Soc., 94, 779 (1972).
8) L. Hedberg and K. Hedberg, J. Am. Chem. Soc., 107, 7257 (1985).
9) K. B. Wiberg, W. P. Deiley, F. H. Walker, S. T.Waddell, L. S. Crocker and M. Newton, J. Am. Chem. Soc., 107, 7247 (1985).
10) E, Honegger, H. Huber, E. Heilbronner, W. P. Dailey and K. B. Wiberg, J. Am. Chem. Soc., 107, 7172 (1985).
11) K. B. Wiberg, S. T. Waddell and K.Laidig, Tetrahedron Lett., 27, 1553 (1986).
12) P. Poritzer and k. Jayasuriya, J. Mol. Struct(Theochem)., 135, 245 (1986).
13) R. P. Messmer and P.A. Schultz, J. Am. Chem. Soc., 108, 7407 (1986).
14) D. Feller and E. R. Davidson, J. Am. Chem. Soc., 109, 4133 (1987).
15) C. Edmiston and K. Ruedenberg, Rev. Mod. Phys., 35, 457 (1963).
16) C. C. J. Roothaan, Rev. Mod. Phys., 23, 69 (1951).
17) W. J. Hehre, R. F. Stewart and J. A. Pople, J. Chem. Phys., 51, 2657 (1969).
18) W. J. Hehre, W. A. Lathan, R. Ditchfield, M. D. Newton and J. A. Pople, GAUSSIAN 70, Program No. 216, Quantum Chemical Program Exchange, Indiana University, Bloomington, Indiana.
19) A. Imamura, Molec. Phys.,15, 225 (1968).